Radiation Dosimetry for Bolus Administration of Oxygen-15-Water

Claude Brihaye, Jean-Claude Depresseux and Dominique Comar

Centre de Recherches du Cyclotron, Université de Liège, Liège, Belgium

We describe the development of a biokinetic model which permits an estimation of organ activities and the dosimetry of a bolus of ^{15}O-water. The aim of this study was to estimate time-activity functions and deduce the cumulated activities in different organs so that the radiation absorbed dose values can be estimated. **Methods:** The model we used includes the right heart chambers, lungs, left heart chambers, brain, liver, kidneys, muscles, gastrointestinal tract and the remainder of the body. Activity in an organ will decay by physical decay with the decay constant, λ, and can diffuse in the organ. An exception is the heart, where blood is ejected from the heart chambers. Depending on the location of the organ in relation to the blood sampling point, organ activities can be calculated by convolution or deconvolution. **Results:** The radiation absorbed dose values were estimated and an effective dose equivalent H_E of 1.16 μSv/MBq (4.32 mrem/mCi) as well as an effective dose E of 1.15 μSv/MBq (4.25 mrem/mCi) were calculated. The cumulated activities in select organs measured by PET gave good agreement with the values calculated by this model. **Conclusion:** The values of effective dose equivalent and effective dose for bolus administration of ^{15}O-water calculated from the absorbed doses estimated by the proposed kinetic model are almost three times higher than those previously published. A total of 8700 MBq (235 mCi) of ^{15}O-water can be administered if an effective dose of 10 mSv (1 rem) is accepted.

Key Words: dosimetry; biokinetic model; oxygen-15-water; effective dose equivalent

J Nucl Med 1995; 36:651–656

Oxygen-15 (half-life, 123 sec; 100% β^+ decay) labeled water (*1*) is widely used to evaluate regional cerebral blood flow using PET (*2–11*) and was proposed for the evaluation of regional pulmonary (*12*), myocardial (*13–14*) and peripheral muscular (*15*) blood flow.

The ^{15}O-water tracer is widely available in PET centers and the short half-life of ^{15}O-water permits repeat measurements in a single session. The diffusion of ^{15}O-water across the blood-brain barrier is considered as acceptable (*16*), and a side method to evaluate regional oxygen extraction rate is available (*3,7,17–19*).

Oxygen-15-water is administered intravenously, with a time profile depending on the chosen numerical method for data processing, which includes short bolus administration in the autoradiographic (*4*) and bolus pluriparametric approaches (*6,7,20*), or ramp administration in the dynamic-integral combined approach (*11*).

The absorbed doses from ^{15}O-water were estimated by Kearfott (*21*) on the basis of a tracer distribution proportional to the water content of different organs and of the whole body. This model should only be applicable, however, if the tracer was administered at a rate allowing permanent steady-state equilibrium.

Since kinetic methods are based on a model where ^{15}O-water distributes as a function of blood flow rather than the volume of water distribution (*22,23*), the current work proposes a reexamination of the Kearfott dose estimates in dynamic conditions, and proposes a new method to more accurately estimate the organ dose values.

MATERIALS AND METHODS

General Considerations

Due to the short half-life of ^{15}O, the dosimetry of a bolus of ^{15}O-water can be estimated principally on the basis of a kinetic model (Fig. 1). After injection, the bolus of activity passes through the right heart chambers, the lungs and the left heart chambers with corresponding input concentrations of C1(t), C2(t) and C3(t) (in μCi/ml). The activities in these organs are q1(t), q2(t) and q3(t) (in μCi), respectively. The input concentration for the brain, kidneys, liver, muscles, gastrointestinal tract and remainder of the body is C4(t) (in μCi/ml). The only parameter that can be measured is the variation of the concentration C4(t) obtained by sampling arterial blood at different times from a catheter introduced into the radial artery. In this model, the recirculation of the blood is taken into account.

For a single organ, i, the quantity of radioactivity $q_i(t)$ (in μCi) present in the organ as a function of time is the product of the convolution of the input function $F_iC_i(t)$ (μCi/sec) and $\mathcal{D}_i(t)$ (no unit), where F_i is the blood flow (ml/sec) to the organ i and $C_i(t)$ (μCi/ml) is the input concentration to the organ i at time t. The function $\mathcal{D}_i(t)$ (no unit) is a function of diffusion of water in the organ according to the Kety model (*23*). The Kety model can be used for all organs except the heart chambers. The model equa-

Received Mar. 17, 1994; revision accepted Sept. 30, 1994.

For correspondence or reprints contact: Claude Brihaye, PhD, Université de Liège, CRC B30, B-4000 Liège, Belgium.

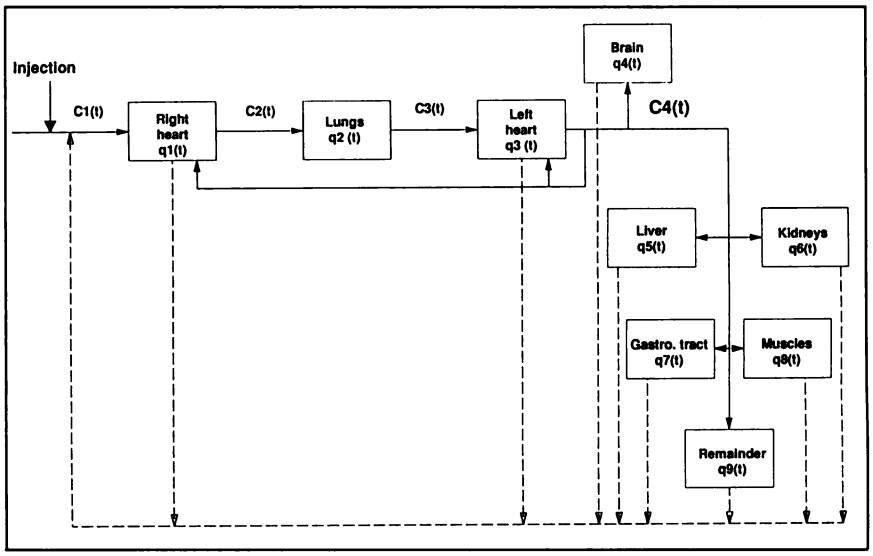

FIGURE 1. Kinetic model of the transit of a ^{15}O-water bolus.

tions are presented in Appendix 1, and the definitions of the symbols used in the biokinetic model are given in Table 1.

Due to the short half-life of ^{15}O, the radiation absorbed dose during the transit of activity through the heart is strongly dependent on residence time in the heart chambers. We developed a realistic beat-by-beat model for cardiac output that is presented in the Appendix. The function $\mathcal{D}_{heart}(t)$ (no unit), which is represented as $\mathcal{D}_{r.heart\ cham}(t)$ for the right heart chambers and $\mathcal{D}_{l.heart\ cham}(t)$ for the left heart chambers, was obtained for the heart chambers by numeric simulation of blood pool ejection to account for ejection occurring in the last third of chamber contraction following an exponential function with decay constant, σ (sec^{-1}). During the first two-thirds of the heart beat, only the physical decay has to be considered (Fig. 2).

Calculation of Time-Activity Variations in the Organs

In this study, we used the blood flow values F_i (ml/sec) (*24*) which are summarized in Table 2, and the experimental functions C4(t), which are an average of the values for six patients.

From the values of C4(t) as a function of time, which can be considered as the output function from the left heart chambers, the activity $q_i(t)$ in the left heart chambers can be obtained by multiplying C4(t) by the diffusion volume of the organ V_i (ml). The input function $F_iC_i(t)$ can be derived by discrete step-by-step

TABLE 1
Definition of Symbols Used in the Biokinetic Model

Symbol	Name/Description	Unit
λ	Physical decay constant	sec^{-1}
$C_i(t)$	Input concentration to the organ i at time t	μCi/ml
$q_i(t)$	Activity present in the organ i at time t	μCi
F_i	Blood flow to the organ i	ml/sec
$F_iC_i(t)$	Input function to the organ i at time t	μCi/sec
$C_{out,i}(t)$	Output concentration from the organ i at time t	μCi/ml
$\mathcal{D}_i(t)$	Function of diffusion of water in the organ i (except the heart chambers) as a function of time	no unit
q1°	Activity in the heart chambers at time 0 for the first beat	μCi
t_{beat}	Duration of a cardiac beat	sec
t_{ej}	Time of the beginning of the ejection (= 2/3 t_{beat})	sec
$t_{beat\ end}$	Time of the end of a beat	sec
$\mathcal{D}_{heart}(t)$	Function of the blood output from the heart chambers. Specifically, $\mathcal{D}_{r.heart\ cham}(t)$ is for the right heart chambers and $\mathcal{D}_{l.heart\ cham}(t)$ is for the left heart chambers	no unit
σ	Decay constant of the exponential function describing the blood ejection	sec^{-1}
V_i	Diffusion volume of the organ i	ml
C1°	Concentration in the heart chambers at time 0 for the first beat	μCi/ml
V_{diast}	Diastolic volume	ml
$q(t = 0)_n$	Activity in the heart chambers at the beginning of the n^{th} beat	μCi
$q(t = t_{ejec})_n$	Activity in the heart chambers at the beginning of the blood ejection for the n^{th} beat	μCi
$q(t = t_{beat\ end})_n$	Activity in the heart chambers at the end of the n^{th} beat	μCi
EF	Blood ejection fraction from the heart chambers	no unit
$\tilde{A}$	Cumulated activity	μCi-hr
τ	Residence time	hr

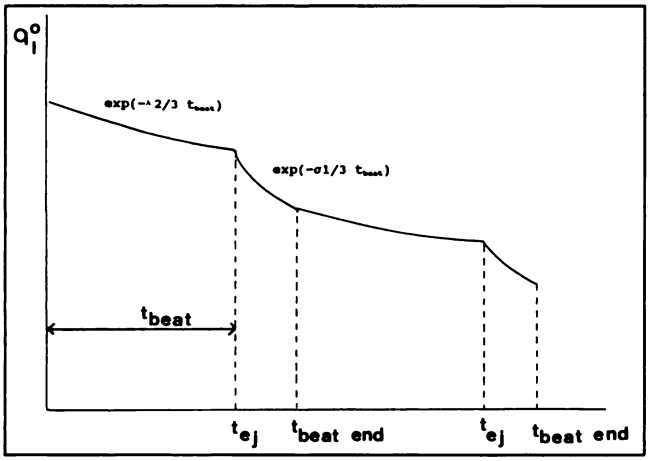

FIGURE 2. Two cycles of blood ejection from the heart chambers.

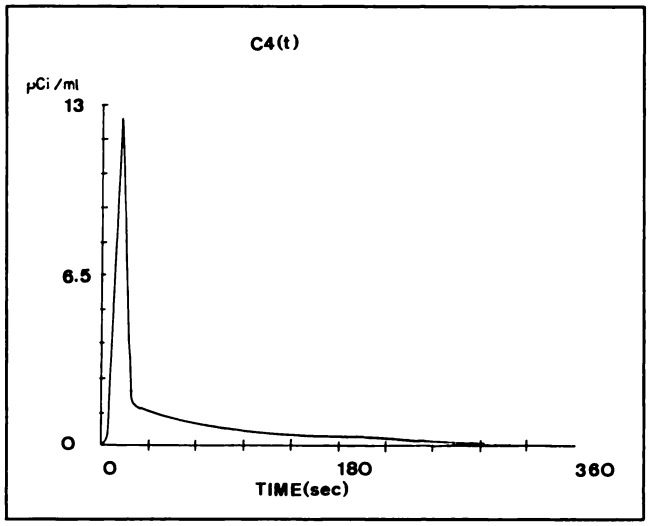

FIGURE 3. Variation of arterial concentration C4(t) as a function of time.

deconvolution of $q_i(t)$ by the function $\mathcal{D}_{i,heart\ chamb}(t)$. Finally, $C_i(t)$ is obtained by dividing $F_iC_i(t)$ by F_i.

$C_i(t)$ for the left heart chambers then becomes the output function $C_{out,i}(t)$ for the preceding organ, which are the lungs, and the same procedure used for the left heart chambers can be applied. The activities $q_i(t)$ at time t are obtained step-by-step for the left heart chambers, lungs and right heart chambers.

For the other organs, including brain, liver, kidneys, gastrointestinal tract, muscles and the remainder of the body, C4(t) is the input concentration $C_i(t)$ and consequently the input function $F_iC_i(t)$ is calculated by multiplying C4(t) by the blood flow F_i. The activities in organ, $q_i(t)$, are derived by discrete convolution of $F_iC4(t)$ by the corresponding function $\mathcal{D}_i(t)$.

Calculation of Cumulated Activities in the Organs

An example of the experimental variation of the activity concentration C4(t) as a function of time is illustrated in Figure 3. Figures 4 and 5 illustrate the calculated curves for the time variations of the quantity of radioactivity q(t) for the organs whose flow rate is measured with ^{15}O-water (i.e., the brain and the heart walls). Due to the convolution process, the origin of the abscissa is shifted from zero to negative values. The cumulated activities $\tilde{A}$ (μCi-hr) were obtained by integrating the functions $q_i(t)$ from zero to infinity. The estimates of the radiation absorbed dose values were calculated using the MIRD technique (*25*). The excess cumulated activity correction (*26*) was used for activity in the remainder of the body. Calculations of the radiation absorbed dose values were then made using the MIRDOSE2 program (*27*).

TABLE 2
Blood Flow Values F_i to Selected Organs*

Organ	F_i (ml/sec)
Brain	12.5
Heart (walls)	4.17
Heart (left chambers)	91.7
(right chambers)	91.7
Lungs	91.7
Liver	21.7
Gastrointestinal tract	16.7
Kidneys	20.0
Muscles	16.7
Remainder of body	0.15–13.3

*See reference 24.

Comparison of Cumulated Activities Calculated Via the Model

To evaluate the accuracy of this model, we compared our calculated cumulated activities with the cumulated activity values estimated experimentally for several organs by PET. These organs included the brain, heart wall, lungs and liver for five patients, and the results were normalized assuming that an activity of 37 MBq was administered. For these studies, a Siemens CTI ECAT 951 R (31 slices) PET camera was utilized. From dynamic acquisitions after injection of ^{15}O-water, the frames visualizing the organs of interest were summed. Regions of interest (ROI) were drawn on the organs and the time-activity curves were then deduced. The integration of these curves from zero to infinity gave the organ cumulated activities.

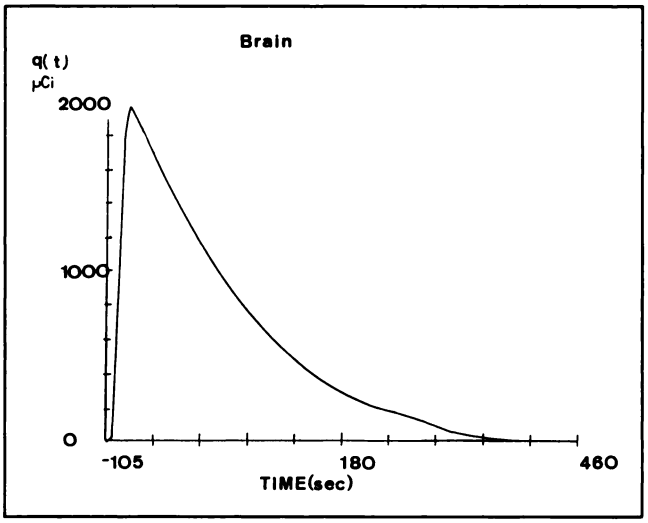

FIGURE 4. Variation of activity q(t) in the brain as a function of time.

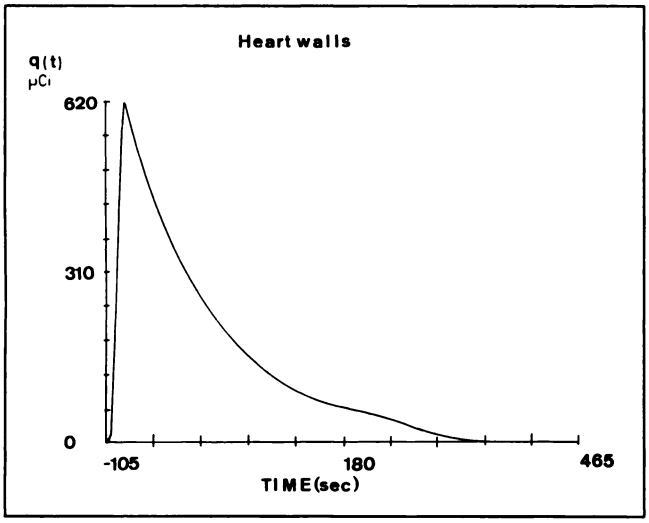

FIGURE 5. Variation of activity q(t) in the heart walls as a function of time.

RESULTS AND DISCUSSION

The values of cumulated activities $\tilde{A}$ (μCi-hr) for administered doses of either 1850 MBq (50 mCi) or 37 MBq (1 mCi) as well as the residence times τ(hr) are presented in Table 3. The estimates of the radiation absorbed dose values are summarized in Table 4. An effective dose equivalent H_E (*28*) of 1.16 μSv/MBq (4.32 mrem/mCi) and an effective dose E (*29*) of 1.15 μSv/MBq (4.25 mrem/mCi) were calculated. The data in Table 5 show a comparison of the values of the cumulated activities $\tilde{A}$ (μCi-hr) in four organs (brain, heart walls, liver and lungs) for 37 MBq administered, measured by PET and calculated via the kinetic model. Good agreement is shown in view of differences in various physiological parameters (organ volume, organ mass, organ blood flow) and the equivalent parameters adopted in the kinetic model. Furthermore, PET evaluation of cumulated activities in the heart walls is underestimated because of the magnitude of the partial volume effect.

Table 4 compares our results and the absorbed dose values published earlier by Kearfott (*21*). These earlier studies used a different model and an effective dose equivalent H_E of 0.50 μSv/MBq (1.84 mrem/mCi) can be calculated from the data of radiation absorbed doses presented in this study. Our results are more realistic; we assume that ^{15}O-water is a blood flow tracer and not a volume tracer. The value of effective dose equivalents calculated in the present work is almost three times higher than the value estimated from Kearfott data. This difference should have a significant implication on the activities of ^{15}O-water routinely administered.

During the time period when this manuscript was being revised, an abstract was published on the same subject (*31*). The absorbed doses in both works were of the same order of magnitude. Recently, Smith et al. (*32*) calculated the dosimetry of intravenously administered ^{15}O-labeled water in man on the basis of a similar approach. They calculated an effective dose equivalent of 1.24 μSv/MBq (4.58 mrem/mCi) and an effective dose of 1.16 μSv/MBq

TABLE 3
Cumulated Activities $\tilde{A}$ for 1850 or 37 MBq Doses

Organ	$\tilde{A}$ (1850 MBq)	$\tilde{A}$ (37 MBq)	Residence time (hr)
Brain	83.7	1.67	0.00167
Heart (walls)	20.97	0.419	0.000419
Liver	120.4	2.41	0.00241
Kidneys	26.30	0.526	0.000526
Muscles	221.0	4.42	0.00442
Gastrointestinal tract	81.9	1.64	0.00164
Remainder	1800.0	36.1	0.035
Left heart (cham)	20.8	0.416	0.000416
Lungs	50.5	1.01	0.00101
Right heart (cham)	19.7	0.39	0.00039
Total body	2445.0	49.0	0.049

TABLE 4
Absorbed Dose Estimates for the Adult in μGy/MBq (mRad/mCi)

Organ	Radiation absorbed dose	
	Present study	Kearfott (*21*)
Brain	0.71 (2.63)	0.16 (0.58)
Breast	1.16 (4.28)	—
GB Wall	1.20 (4.45)	—
Lower large intestine	1.54 (5.68)	0.59 (2.2)
Small intestine	1.05 (3.90)	0.57 (2.1)
Stomach	1.21 (4.46)	0.57 (2.1)
Upper large intestine	1.26 (4.66)	0.57 (2.1)
Heart Wall	0.67 (2.49)	0.57 (2.1)
Kidneys	0.95 (3.52)	0.57 (2.1)
Liver	0.75 (2.76)	0.54 (2.0)
Lungs	0.57 (2.10)	0.54 (2.0)
Muscle	0.15 (0.57)	0.54 (2.0)
Ovaries	1.79 (4.39)	0.57 (2.1)
Pancreas	1.21 (4.48)	0.54 (2.0)
Red marrow	1.49 (5.51)	0.32 (1.2)
Bone surface	1.12 (4.14)	0.21 (0.78)
Skin	1.07 (3.94)	0.57 (2.1)
Spleen	1.19 (4.41)	0.57 (2.1)
Testes	1.11 (4.11)	0.59 (2.2)
Thyroid	1.11 (4.09)	0.51 (1.9)
UB Wall	1.16 (4.31)	0.35 (1.3)
Uterus	1.20 (4.44)	0.51 (1.9)
Total Body	0.42 (1.55)	0.43 (1.6)

TABLE 5
Comparison of PET and the Kinetic Model Mean Cumulated Activities, $\tilde{A}$ (μCi-hr), for a 37-MBq Dose

Organ	$\tilde{A}$ measured by PET	$\tilde{A}$ calculated
Brain	2.0 ± 0.5	1.67
Heart walls	1.3 ± 0.9	0.42
Liver	3.4 ± 0.6	2.41
Lungs	1.0 ± 0.3	1.01

(4.29 mrem/mCi), which are in good agreement with the values presented in this work.

CONCLUSIONS

In this work, we presented a biokinetic model describing the distribution of a bolus of ^{15}O-labeled water. This model is based on the distribution of ^{15}O-water as a blood flow tracer and not a volume tracer.

From the time-activity functions calculated on the basis of the model, the cumulated activities in different organs were estimated and the radiation absorbed dose values were calculated. An effective dose equivalent H_E of 1.16 μSv/MBq (4.32 mrem/mCi) and an effective dose E of 1.15 μSv/MBq (4.25 mrem/mCi) were calculated. These values are almost three times higher than the values calculated from data previously published.

A total of 8700 MBq (235 mCi) of ^{15}O-water can be administered if an effective dose of 10 mSv (1 Rem) is accepted. This effective dose value can be compared with the values for other PET studies (*30*) such as ^{18}F-FDG, 370 MBq (10 mCi) = 3.7 mSv (370 mrem) and ^{11}C-spiperone, 925 MBq (25 mCi) = 4.9 mSv (490 mrem).

APPENDIX: EQUATIONS FOR WATER DIFFUSION AND BLOOD EJECTION CYCLES

Equations Describing the Diffusion of Water in Organ i

$$q_i(t) = F_i C_i(t) \circledast \mathcal{D}_i(t) \qquad \text{Eq. A1}$$

where F_i (ml/sec) is the blood flow rate to the organ i; $C_i(t)$ (μCi/ml) is the input concentration to the organ i; $\circledast$ is the symbol of convolution; $\mathcal{D}_i(t)$ is the diffusion function; = exp [(−F_i/V_i + λ)t]; and V_i is the diffusion volume in the organ i. Moreover,

$$C_{out,i}(t) = q_i(t)/V_i, \qquad \text{Eq. A2}$$

where $C_{out,i}(t)$ is the output concentration from the organ i. Taking into account the physical decay during the transit between the organ i and the next organ i + 1, the concentration $C_{out,i}$ becomes the input concentration for the next organ i + 1 if there is no blood branching between the two organs, which gives the following relationship:

$$C_{i+1}(t) = C_{out,i}(t). \qquad \text{Eq. A3}$$

Equations for Ejection of Blood from the Heart Chambers

Two cycles of blood ejection from the heart chambers were presented in Figure 2. The duration of one beat t_{beat}(sec) can be divided in two parts: (1) during the first two-thirds of the duration of the beat, there is no ejection and the activity decays physically with the decay constant λ (sec^{-1}); and (2) during the last third, blood is ejected with the ejection decay constant σ (sec^{-1}).

Equations for the First Beat. The activity present in the heart chambers at time 0 for the first beat, $q(t = 0)_1$ (μCi), is the product of the concentration present in the heart chambers $C1^0$ (μCi/ml) and the diastolic volume V_{diast} (in ml):

$$q(t = 0)_1 = C1° \, V_{diast}. \qquad \text{Eq. A4}$$

For the period of time between 0 and the beginning of the ejection (t_{ej}), which corresponds to the first two-thirds of the duration of the beat, only the physical decay has to be considered:

$$q(t = t_{ej})_1 = C1° \, V_{diast} \exp(-\lambda 2/3 t_{beat}). \qquad \text{Eq. A5}$$

As long as the blood ejection occurs effectively (period of time between t_{ejec} and $t_{beat\ end}$, corresponding to the last third of the duration of the beat), the blood is ejected following an exponential function with the ejection decay constant σ (sec^{-1}).

$$q(t = t_{beat\ end})_1 = C1° \, V_{diast} \exp(-\lambda 2/3 t_{beat}) \exp(-\sigma 1/3 t_{beat}). \qquad \text{Eq. A6}$$

Since at the end of the beat, the blood fraction remaining in the chambers is (1 − EF), where EF is ejection fraction, the activity present in the chambers at the end of the beat ($t = t_{beat\ end}$) is given by the relationship:

$$q(t = t_{beat\ end})_1 = q(t = t_{ej})_1 (1 - EF), \qquad \text{Eq. A7}$$

where EF is ejection fraction.

It follows that:

$$C1° \, V_{diast} \exp(-\lambda 2/3 t_{beat})(1 - EF) = C1° \, V_{diast} \exp(-\lambda 2/3 t_{beat}) \exp(-\sigma 1/3 t_{beat}), \qquad \text{Eq. A8}$$

which can be simplified in:

$$(1 - EF) = \exp(-\sigma 1/3 t_{beat}), \qquad \text{Eq. A9}$$

from which the constant σ can be extracted:

$$\sigma = -\frac{1}{1/3 t_{beat}} \ln(1 - EF). \qquad \text{Eq. A10}$$

Equations for the Second Beat. The same considerations can be applied and it follows that:

$$q(t = 0)_2 = C1° \, V_{diast} \exp(-\lambda 2/3 t_{beat}) \exp(-\sigma 1/3 t_{beat}), \qquad \text{Eq. A11}$$

$$q(t = t_{ej})_2 = C1° \, V_{diast} \exp(-\lambda 2/3 t_{beat}) \exp(-\sigma 1/3 t_{beat}) \times \exp(-\lambda 2/3 t_{beat}), \qquad \text{Eq. A12}$$

$$q(t = t_{beat\ end})_2 = C1° \, V_{diast} \exp(-\lambda 2/3 t_{beat}) \exp(-\sigma 1/3 t_{beat}) \times \exp(-\lambda 2/3 t_{beat}) \exp(-\sigma 1/3 t_{beat}). \qquad \text{Eq. A13}$$

Equations for the n^{th} Beat.

$$q(t = t_{beat\ end})_n = C1° \, V_{diast} [\exp(-\lambda 2/3 t_{beat})]^n [\exp(-\sigma 1/3 t_{beat})]^n \qquad \text{Eq. A14}$$

with

$$\sigma = -\frac{1}{1/3 t_{beat}} \ln(1 - EF). \qquad \text{Eq. A15}$$

After normalizing to q1° (= $C1° \, V_{diast}$) = 1, which is the activity in the heart chambers at time 0 for the first beat, the final equation giving the ratio of the activity present in the heart chambers to the initial activity, i.e., the value of $\mathcal{D}_{heart}(t = t_{beat\ end})_n$ at the end of the n^{th} beat, is:

$$\mathcal{D}_{heart}(t = t_{beat\ end})_n =$$

$$[\exp(-\lambda 2/3t_{beat})]^n [\exp(-\sigma 1/3t_{beat})]^n \quad \text{Eq. A16}$$

with

$$\sigma = -\frac{1}{1/3t_{beat}} \ln(1 - EF). \quad \text{Eq. A17}$$

We adopted a cardiac pulsation of 85 bpm (t_{beat} = 0.71 sec). The functions $\mathcal{D}_{heart}(t)$, which are symbolized $\mathcal{D}_{r.heart\ cham}(t)$ and $\mathcal{D}_{l.heart\ cham}(t)$ for the right heart chambers and the left heart chambers, respectively, were calculated using this last equation step-by-step with an increment unit of 0.71 sec and taking values of 60% for the right heart and 65% for the left heart for ejection fraction.

REFERENCES

1. Welch MJ, Lifton JT, Ter-Pogossian MM. Preparation of millicurie quantities of oxygen-15 labeled water. *J Labd Compd Radiopharm* 1969;5:168–172.
2. Ter-Pogossian MM, Eichling JO, Davis DO. The determination of regional cerebral blood flow by means of water labeled with radioactive oxygen-15. *Radiology* 1969;93:31–40.
3. Frackowiak RSJ, Lenzi G, Jones T, Heather JD. Quantitative measurement of regional cerebral blood flow and oxygen metabolism in man using ^{15}O and positron emission tomography: theory, procedure and normal values. *J Comp Assist Tomogr* 1980;4:727–736.
4. Raichle ME, Martin WRW, Herscovitch P, Mintun MA, Markham J. Brain blood flow measured with intravenous $H_2{}^{15}O$. II. Implementation and validation. *J Nucl Med* 1983;24:790–798.
5. Herscovitch P, Raichle ME. Brain blood flow measured with intravenous $H_2{}^{15}O$. I. Theory and error analysis. *J Nucl Med* 1983;24:782–789.
6. Huang SC, Carson RE, Hoffman EJ, Mac Donald N, Barrio JR, Phelps ME. Quantitative measurement of local cerebral blood flow in humans by positron computed tomography and ^{15}O-water. *J Cereb Blood Flow Metab* 1983;3:141–153.
7. Depresseux JC, Cheslet JP, Franck G. An original method for the concomitant tomographic assessment of cerebral blood flow, oxygen extraction rate, blood volume and exchangeable water volume in man. *J Cereb Blood Flow Metab* 1983;3(suppl 1):152–153.
8. Ginsberg MD, Howard BE, Hassel WR. Emission tomographic measurement of local cerebral blood flow in humans by an in vivo autoradiographic strategy. *Ann Neurol* 1984;15:S12–S18.
9. Kanno I, Lammertsma AA, Heather JD, Gibbs JM, Rhodes CG, Clark JC, Jones T. Measurement of cerebral blood flow using bolus inhalation of $C^{15}O_2$ and positron emission tomography: description of the method and its comparison with $C^{15}O_2$ continuous inhalation method. *J Cereb Blood Flow Metab* 1984;4:224–234.
10. Lammertsma AA, Frackowiak RSJ, Hoffman JM, et al. The $C^{15}O_2$ build-up technique to measure regional cerebral blood flow and volume of distribution of water. *J Cereb Blood Flow Metab* 1989;9:461–470.
11. Lammertsma AA, Cunningham VJ, Deiber MP, et al. Combination of dynamic and integral methods for generating reproducible functional CBF images. *J Cereb Blood Flow Metab* 1990;10:675–686.
12. Schuster DP, Mintun MA, Green MA, Ter-Pogossian MM. Regional lung water and hematocrit determined by positron emission tomography. *J Appl Physiol* 1985;59:860–868.
13. Iida H, Kanno I, Takahashi A, et al. Measurement of absolute myocardial blood flow with $H_2{}^{15}O$ and dynamic positron emission tomography: strategy for quantification in relation to the partial volume effect. *Circulation* 1988; 78:104–115.
14. Iida H, Rhodes CG, De Silva R, et al. Use of the left ventricular time-activity curve as a noninvasive input function in dynamic oxygen-15 water positron emission tomography. *J Nucl Med* 1992;33:1669–1677.
15. Depairon M, Depresseux JC, Zicot M. Quantitation of regional muscle blood flow and oxygen uptake in peripheral arterial insufficiency using positron emission tomography. *Clin Hemorheol* 1988;8:385–390.
16. Herscovitch P, Raichle ME, Kilbourn MR, Welch MJ. Positron emission tomographic measurement of cerebral blood flow and permeability-surface area product of water using (^{15}O)water and (^{11}C)butanol. *J Cereb Blood Flow Metab* 1987;7:527–542.
17. Raichle ME, Larson KB, Markham J, Depresseux JC, Grubb RL, Ter-Pogossian MM. Measurement of regional oxygen consumption by positron emission tomography. *J Cereb Blood Flow Metab* 1981;1(suppl 1):7–8.
18. Mintun MA, Raichle ME, Martin WRW, Herscovitch P. Brain oxygen utilization measured with ^{15}O radiotracers and positron emission tomography. *J Nucl Med* 1984;25:177–187.
19. Ohta S, Meyer E, Thompson CJ, Gjedde A. Oxygen consumption of the living human brain measured after a single inhalation of positron emitting oxygen. *J Cereb Blood Flow Metab* 1992;12:179–192.
20. Iida H, Kanno I, Miura S, Murakami M, Takahashi K, Uemura K. Error analysis of a quantitative cerebral blood flow measurement using $H_2{}^{15}O$ autoradiography and positron emission tomography, with respect to the dispersion of the input function. *J Cereb Blood Flow Metab* 1986;6:536–545.
21. Kearfott KJ. Absorbed dose estimates for PET: $C^{15}O$, ^{11}CO and $CO^{15}O$. *J Nucl Med* 1982;23:1031–1037.
22. Harper PV. Potentials and problems of short-lived radionuclides in medical imaging applications. *Int J Appl Rad Isot* 1977;28:5–11.
23. Kety SS, Schmidt CF. Nitrous oxide method for the quantitative determination of cerebral blood flow in man: theory, procedure and normal values. *J Clin Invest* 1948;27:475–483.
24. Wright S. *Physiologie appliquée à la médecine*. Paris: Flammarion Médecine-Sciences; 1980.
25. Loevinger R, Berman M. A revised schema for calculating the absorbed dose from biologically distributed radionuclides. *MIRD pamphlet no. 1, revised.* New York, NY: Society of Nuclear Medicine; 1976.
26. Cloutier RJ, Watson EE, Roher RH, Smith EM. Calculating the radiation dose to an organ. *J Nucl Med* 1973;14:53–55.
27. Watson EE, Stabin MG, Bolch WE. MIRDOSE2 program, Oak Ridge Associated Universities; 1984.
28. ICRP. *Recommendations of the ICRP*. Annals of the ICRP, 1. Publication 26; 1977.
29. ICRP. *The 1990 Recommendations of the Commission*. Annals of the ICRP, 21. Publication 60; 1991.
30. Johansonn L, Mattsson S, Nosslin B, Leide-Svegborn S. Effective dose from radiopharmaceuticals. *Eur J Nucl Med* 1992;19:933–938.
31. Herscovitch P, Carson RE, Stabin M, Stubbs JB. A new kinetic approach to estimate the radiation dosimetry of flow-based radiotracers. *J Nucl Med* 1993;34:155–156P.
32. Smith T, Tong C, Lammertsma AA, et al. Dosimetry of intravenously administered ^{15}O-labelled water in man: a model based on experimental human data from 21 subjects. *Eur J Nucl Med* 1995;21:1126–1134.